

# Chlorite chemical refinement during giant quartz vein formation

Eloi González-Esvertit<sup>1,2,3\*</sup>, Àngels Canals<sup>1</sup>, Paul D. Bons<sup>4,5</sup>, Josep Maria Casas<sup>6</sup>, Fernando Nieto<sup>7</sup> and Enrique Gomez-Rivas<sup>1</sup>

<sup>1</sup>*Departament de Mineralogia, Petrologia i Geologia Aplicada, Facultat de Ciències de la Terra, Universitat de Barcelona. Barcelona 08028, Spain.*

<sup>2</sup>*Institut de Recerca Geomodels, Universitat de Barcelona. Barcelona 08028, Spain.*

<sup>3</sup>*Geosciences Barcelona (GEO3BCN-CSIC). Barcelona 08028, Spain.*

<sup>4</sup>*Department of Geosciences, Tübingen University. Tübingen 72076, Germany.*

<sup>5</sup>*China University of Geosciences (Beijing). Beijing 100083, China.*

<sup>6</sup>*Departament de Dinàmica de la Terra i l'Oceà, Facultat de Ciències de la Terra, Universitat de Barcelona. Barcelona 08028, Spain.*

<sup>7</sup>*Departamento de Mineralogía y Petrología, Instituto Andaluz de Ciencias de la Tierra, Universidad de Granada-CSIC. Granada 18002, Spain.*

\* *Corresponding author:* [e.gonzalez-esvertit@ub.edu](mailto:e.gonzalez-esvertit@ub.edu)

---

## **This is a postprint version of the article:**

González-Esvertit, E., Canals, À., Bons, P. D., Casas, J. M., Nieto, F., & Gomez-Rivas, E. (2024).

Chlorite chemical refinement during giant quartz vein formation. *GSA Bulletin* (2024), 136 (11-12): 5208–5216. <https://doi.org/10.1130/B37510.1>

## **The published copy-edited version can be found at:**

<https://pubs.geoscienceworld.org/gsa/gsabulletin/article-abstract/136/11-12/5208/644576/Chlorite-chemical-refinement-during-giant-quartz>

## **ABSTRACT**

The major elemental composition of chlorite is widely used for petrogenetic investigations on low-temperature geological processes. However, compositional variations of chlorite within a given tectonic environment are common and, when overlooked, can lead to erroneous petrological interpretations. We thoroughly investigate chlorites occurring within Giant Quartz Veins (GQVs) in the basement rocks of the Pyrenees. These structures have widths of up to tens of metres and lengths of kilometres, and form in both mid-crustal ductile and upper-crustal seismogenic domains. Texturally constrained chlorite analyses and spatially resolved whole-rock elemental analysis reveal a progressive chemical evolution of chlorite coupled to GQV formation. Six chlorite generations that were distinguished according to their texture show consistent chemical variations at the microscale. Host rock- and quartz vein-related chlorites are the textural and compositional endmembers. Between them, a progressive chemical refinement occurred in transitional chlorite compositions linked to host rock, vein quartz, and pressure-solution microstructures, in accordance with significant fluid-rock interactions leading to GQV formation. This rock alteration process is further confirmed at the macroscale by the progressive depletion of all major and trace elements but silica, with decreasing distance towards GQVs. We demonstrate that (i) inferring the temperature conditions of chlorite crystallization is not as straightforward as generally assumed, and that (ii) giant quartz veins can be formed under rock-buffered conditions, at lower temperatures than previously thought. These results have implications for the practice commonly used in chlorite-based geothermometry, as well as for the modes of fluid, heat, and mass transport within the Earth's crust.

## 1 INTRODUCTION

Estimating the temperature at which geological processes occur, *i.e.*, geothermometry, is key to understanding fluid and mass transfer and rock deformation mechanisms in the Earth's crust, which control the tectono-sedimentary and tectono-metamorphic evolution of basins and orogens, as well as the formation of ore deposits (Holland, 1965; Chapman, 1986; Brown, 1995; Gomez-Rivas et al., 2020). Geothermometry is based on index minerals and mineral assemblages (Fyfe et al., 1958), fluid inclusion studies (Roedder, 1984), fabric analysis (Hirth and Tullis, 1992), cation exchange processes (Anderson et al., 2008), and isotopic fractionation (Valley, 2001), among other approaches. Many of these methods are, however, not applicable at low temperatures ( $T < 350^{\circ}\text{C}$ ) due to mineral phase stability, deformation conditions, and kinetic concerns. Chlorite, a mineral group including up to 13 mineral species that can be found in a great variety of rocks and geological environments, has been used for decades for such purposes in different low-temperature processes. Since the chemical composition of chlorite depends on the temperature, pressure, and redox conditions of crystallization among others (de Caritat et al., 1993), several empirical equations have attempted to relate chlorite chemical composition with its temperature of growth (see a review in the Supplemental Material 1, SM1; Fig. S1, S2). However, such empirical approaches are not based on equilibrium reactions and, therefore, are only valid for the specific context for which they were calibrated, often yielding unreliable results (Essene and Peacor, 1995).

More recently, semi-empirical and thermodynamic open-source chlorite geothermometers have been established as robust approaches for low-temperature geothermometry (Bourdelle et al., 2013; Lanari et al., 2014; Inoue et al., 2018) (SM1; Fig. S1, S2). These methods are based on the activity of compositional endmembers under quartz-chlorite equilibrium to infer the growth temperature of a given crystal. Therefore, they do not depend on any site-specific calibration, and

provide reliable results for a wide range of chlorite compositions in different geological settings (e.g., Essene and Peacor, 1995; Bourdelle and Cathelineau, 2015; Masci et al., 2019; Bourdelle, 2021). The rising popularity of these modern approaches is due to the relative ease of data acquisition (major element composition with an Electron Microprobe; EMP) and, in some cases, due to straightforward calculations with open-source graphical tools or automated spreadsheets (e.g., Bourdelle and Cathelineau, 2015; Verdecchia et al., 2019). Accordingly, chlorite thermometry is nowadays a versatile approach, commonly used as an exploration vector towards concealed orebodies (Wilkinson et al., 2015) or geothermal fields (Uno et al., 2023). Furthermore, it has also been widely used for inferring rock thermal histories, providing insights into the temperature of metamorphism (e.g., Verdecchia et al., 2019; Rajič et al., 2023), fluid flow (e.g., Miron et al., 2013; Rasmussen et al., 2020), and brittle and ductile deformation (e.g., Torgersen and Viola, 2014; Menegon and Fagereng, 2021).

The chemical composition of chlorite is known to strongly vary within the same tectonic environment of growth, even at the nanoscale, due to local diffusional and dissolution-precipitation processes or changes in pressure, temperature and fluid composition (Wagner and Cook, 2000; Bourdelle et al., 2018; Pérez-Cáceres et al., 2020; Rajič et al., 2023). These variations lead to the formation of different types of chlorites within the same setting, potentially yielding different temperatures depending on the analyzed crystal, or even in nanometer-size areas of the same crystal, which indicates a temperature zonation (Bourdelle et al., 2018). However, such variations are often overlooked due to a lack of systematic textural groundwork prior to analysis, resulting in biased interpretations, averaged compositions, and mixed temperature estimates for different processes, such as hydrocarbon or geothermal energy exploration and ore deposit formation. In the field of fluid inclusions, for example, the paradigm-shifting Fluid Inclusion

Assemblage approach changed the most elementary procedures by which fluid inclusions are grouped and results are interpreted (*e.g.*, Goldstein, 2001; Fall and Bodnar, 2018), allowing to settle on a systematic workflow that is nowadays followed in laboratories worldwide. However, a similar breakthrough approach has not been implemented yet to systematically identify the most finely discriminated, petrographically associated groups of chlorites that have grown at the same time, allowing data to be placed in a well-defined spatiotemporal context before deducing its petrogenetic significance.

We address this problem by investigating chlorites associated with the formation of Giant Quartz Veins (GQVs), which are up to tens of metres wide and kilometres long and occur worldwide (*e.g.*, Jia and Kerrich, 2000; González-Esvertit et al., 2022a). Some are related to economically important ore deposits, such as orogenic gold (Goldfarb et al., 2001), and/or to zones of localised deformation, such as brittle faults, shear zones or fold axial planes. However, their fluid sources, fluid transport mechanisms, and the tectonic and geochemical controls on their formation remain debated hitherto (Bons et al., 2022). A consistent, progressive variation of textures, compositions, and formation temperatures of different chlorite generations, at the  $\mu\text{m}$ -mm scale, coupled with spatially resolved whole-rock geochemical variations, at the kilometre scale, provide a word of caution about chlorite thermometry and reveal new insights on the formation of GQVs. The analysis presented here is based on GQVs from the Pyrenees, an Alpine chain involving pre-Variscan (late Neoproterozoic to Carboniferous) and Variscan (Carboniferous to Permian) basement rocks that represents a rich and diverse region in terms of GQV occurrence in different host rock types (González-Esvertit, 2022a). Accordingly, the results of this study also have implications for the regional tectono-thermal evolution of the Pyrenees, from Variscan to Alpine (late Cretaceous to Miocene) times.

## 2 GEOLOGICAL SETTING

The Pyrenean chain (SW Europe; Fig. 1) was formed due to the collision of the Iberian and Eurasian plates from the late Cretaceous to the Miocene (Muñoz, 1992). Three major Alpine thrusts, from bottom to top named Rialp-(Canigó), Orri-(Cadí), and Pedraforca-(Noguères), formed an antiformal stack in the central and eastern parts of the chain resulting in the exhumation of pre-Variscan and Variscan basement rocks. Cadomian, Sardinic, and Variscan igneous activity, as well as Sardinic, Variscan, and Alpine deformational events and a Variscan regional metamorphism are recorded in these rocks (Muñoz, 1992; Casas, 2010; Aguilar et al., 2014; Navidad et al., 2018; Margalef et al., 2023) (Fig. 1).

More than 700 GQVs hosted by rocks of different age and composition have been identified in the Pyrenees from satellite images and aerial orthophotographs (Figs. 1, S3). An inventory of the distribution, geometry, and statistics of these veins and host rocks is available in the GIVEPY database (<https://givepy.info>; González-Esvertit et al., 2022a). The study area of the present work is located at the southern slope of the E-W-trending Canigó Massif (Fig. 1). It exposes two GQVs hosted by blueish slates of the Lower Cambrian Err Fm. and greenish slates and sandstones with interbedded quartzite layers of the Cambrian-Lower Ordovician Serdinya Fm. (Padel et al., 2018). These veins infer a significant relief in the topography (Fig. 2A; S3) and show a heterogeneous internal structure in terms of grain size, finite strain, and crystal transparency (Fig. 2B, C). Variable phyllosilicate content and highly silicified fragments of metasedimentary rocks are common, becoming more abundant towards the vein edges where the contact with the silicified host rocks is progressive and diffuse. A well-developed crenulation cleavage ( $S_2$ ) is the most recognizable feature in the rocks hosting the studied GQVs (Fig. S4A, B).  $S_2$  is related to outcrop-scale

asymmetric folds affecting bedding surfaces.  $S_2$  occurs as NW-SE-trending and moderately NE-dipping anastomosing surfaces that at the microscopic scale can be described as a crenulation cleavage defined by phyllosilicate orientation and affecting a previously developed  $S_{0-1}$  bedding-parallel cleavage (Fig. S5A, B). Deformation mesostructures further include a meter-spaced joint set and ductile deformation bands with characteristic S-C fabrics with C' shear bands that affect both the GQVs and their host rocks (Fig. 2, S4C). The boundaries of the GQVs show slickensides indicating south-directed movement on an E-W trending, north dipping fault, that postdates the  $S_2$  cleavage. This thrust, of presumed Alpine age (González-Esvertit et al., 2022b, 2023), is similar to other thrusts linked to quartz bodies located northwards of the study area (Fig. 1). Detailed geological maps and a regional summary of the main stratigraphic, structural, and petrographic features of the GQVs and their host rocks in the study area are provided in González-Esvertit et al. (2022b, 2023) and in the SM1 (Figs. S4-S6).

### 3 METHODS

Geological mapping and structural analysis of the study area were carried out to establish the tectonic and stratigraphical framework for petrogenetic investigations at the microscale (SM1; Figs. S4, S5). GQVs and host rock samples were collected to determine spatial variations in texture, microstructure, and chemical composition. Special attention was paid to the evolution of chlorite textures as a function of their position within and adjacent to the GQVs, their related microstructures, and their surrounding mineralogy (Fig. 2C-G; SM1). Various chlorite types with different textural and microstructural features were petrographically distinguished and analysed in an EMP to evaluate microscale geochemical variations during GQV formation. Whole-rock major and trace elements analyses on representative samples collected along a 1 km-long scanline,

oriented normal to the main direction of one of the studied GQVs, were used to constrain macroscale geochemical trends at different distances to the vein quartz. Additional information and descriptions of the analytical procedures are provided in the [SM1](#).

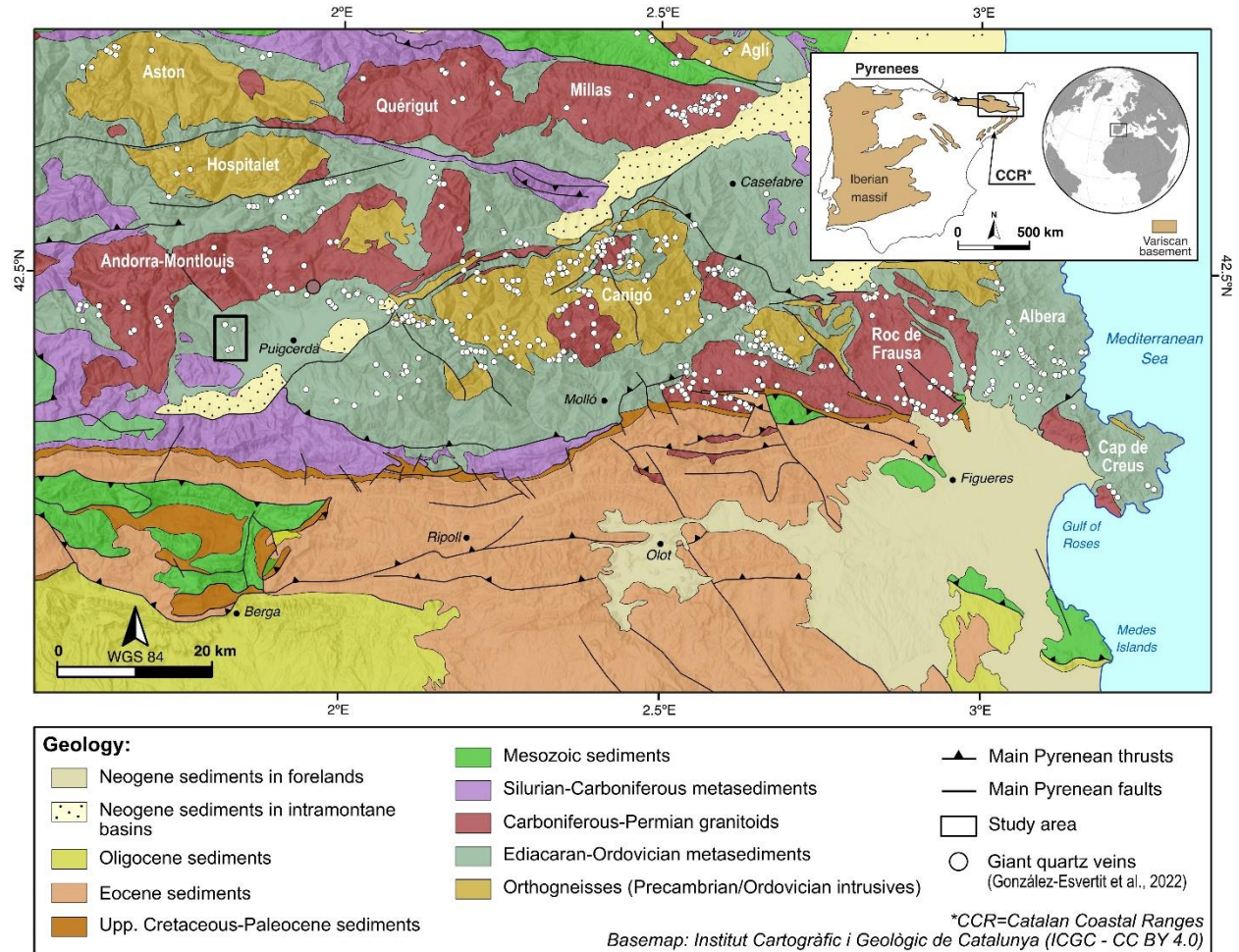


Figure 1. Simplified geological map of the basement and cover rocks cropping out in the Eastern Pyrenees, including the spatial distribution of Giant Quartz Veins provided in [González-Esvertit et al. \(2022a\)](#) and the location of the study area.

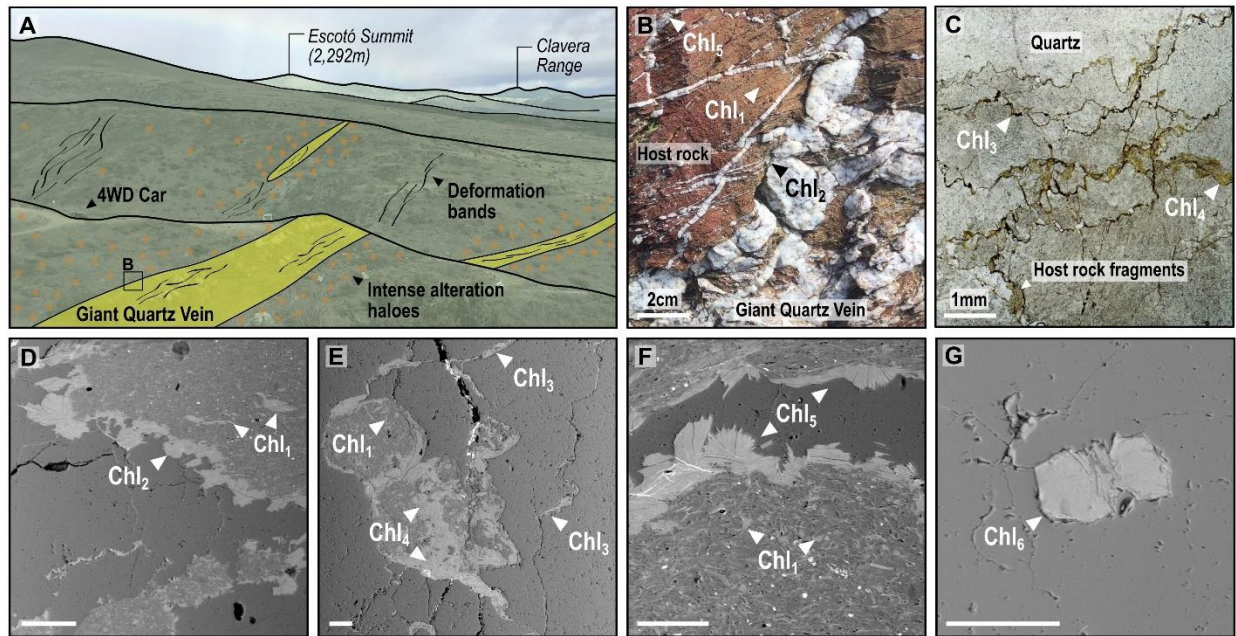


Figure 2. Geological sketch (view towards the East) of the studied Giant Quartz Vein (A), and representative features of the vein boundaries at the outcrop (B) and thin section (C) scales. (D-G) Backscatter electron images of the distinguished chlorite types (Chl<sub>1-6</sub>). Note that different chlorite types often coexist within the same samples. Scalebars in D-G are 100 µm. See the geological background in the SM1 and field photographs of the investigated Giant Quartz Vein in Figure S3. Mineral abbreviations following [Warr \(2021\)](#).

#### 4 RESULTS

Six different chlorite types were petrographically distinguished in 32 representative thin sections of GQVs and their host rocks (Fig. 2D-G, S5, S6). Chl<sub>1</sub> chlorites formed within the host rocks and are the only chlorite type that is not spatially related to vein quartz (Fig. 2B, D-F, S5A, B, S6A). They occur as chlorite-phengite interlayers that form the microlithons of the S<sub>2</sub> crenulation cleavage. Chl<sub>2</sub> chlorites are sub-idiomorphic isometric aggregates composed of diablastic or vermicular-shaped crystals that grow from host rock domains inwards into the GQV quartz (Fig.

2D, S6E). Chl<sub>3</sub> chlorites are present within the GQV quartz as allotriomorphic masses associated with simple wave-like or seismogram pinning type stylolites with variable roughness (Koehn et al., 2016) (Fig. 2C, E, S6D). Chl<sub>4</sub> chlorites occur in altered host rock fragments that are embedded within the GQV quartz. They are found as allotriomorphic or vein-shaped replacing masses ranging from few microns up to four millimetres (Fig. 2C, E). These replacing masses postdate both S<sub>0-1</sub> and S<sub>2</sub> cleavages present in the host rocks (Fig. S5C, D, S6F). Chl<sub>5</sub> chlorite crystals show chrysanthemum-like morphologies and are located along the walls of cm-wide crack-seal quartz veinlets that crosscut the GQV quartz and host rocks (Fig. 2F, S6G). Chl<sub>6</sub> chlorites, which are only found as isolated idiomorphic crystals within undeformed areas of the GQV quartz (Fig. 2G, S6H), represent the opposite end of the spectrum from Chl<sub>1</sub> and are the only type of chlorite that is not spatially related to the host rocks. No chlorites have been identified in high-strain domains within GQVs, where deformation is localized in mylonitic bands dominated by subgrain rotation recrystallization (Fig. S5, S6).

Noteworthy, the chlorite types that we distinguished according to their texture show consistent variations in their chemical composition that reflect cationic exchange processes involving a progressive enrichment of Si, Al<sup>(VI)</sup>, and Ca, and a depletion of Al<sup>(IV)</sup>, Mg, and Fe<sup>T</sup> contents (Fig. 3; see SM2). Chl<sub>1</sub> and Chl<sub>6</sub> chlorites that correspond to the original chlorites formed in the host rocks and to the chlorites isolated within the GQV quartz, respectively, represent the two textural and compositional endmembers. Chl<sub>2-5</sub> chlorite types represent intermediate compositions that reflect a progressive chemical evolution of the system, in agreement with their textural positions that are not related to quartz or host rocks alone, but to both simultaneously (Fig. 2D-G, 3, S5, S6). Outcrop characterization (Fig. 2A, S4) and spatially resolved whole-rock geochemistry of GQV and altered and unaltered host rocks also show a spatially progressive enrichment of SiO<sub>2</sub> (Fig. 4,

SM2). QV samples are mostly composed of SiO<sub>2</sub>, whilst their host rocks sampled more than 600 m away from them show chemical compositions similar to those commonly reported for other unaltered Pyrenean Cambrian-Ordovician metasedimentary rocks (e.g., Bons, 1988). Intermediately, progressive variations of the chemical composition of altered host rocks suggest a continuous depletion of all major and trace elements with decreasing distance towards the main quartz bodies, except for the SiO<sub>2</sub> that increases substantially (Fig. 4; SM2).

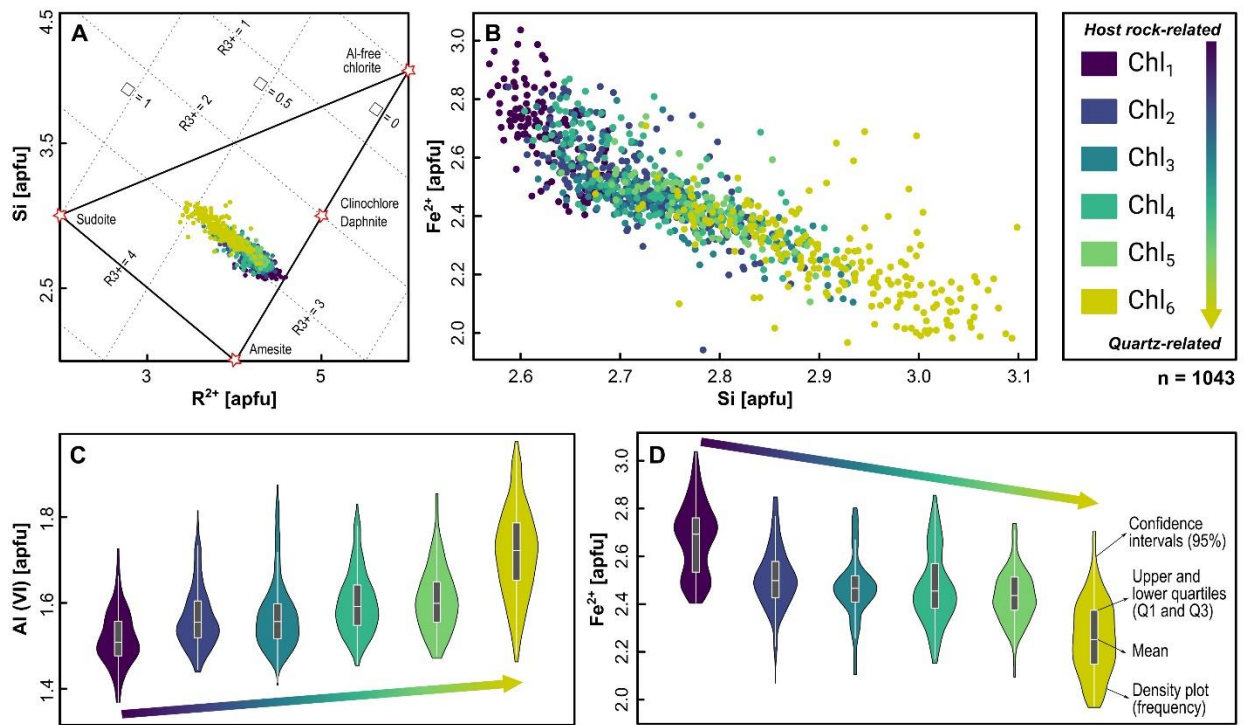


Figure 3. Compositional variations of the studied chlorites regarding their texture and position relative to the giant quartz veins. (A) R<sup>2+</sup> vs. Si classification diagram. (B) Si vs. Fe<sup>(T)</sup> diagram; note the progressive enrichment of Si towards the quartz-related chlorites (from Chl<sub>2</sub> to Chl<sub>6</sub>). (C, D) Violin-box plots of the Al<sup>(VI)</sup> and Fe<sup>(T)</sup> content variations, respectively. See raw data in the SM2. [apfu = atoms per formula unit, normalized to 14O].

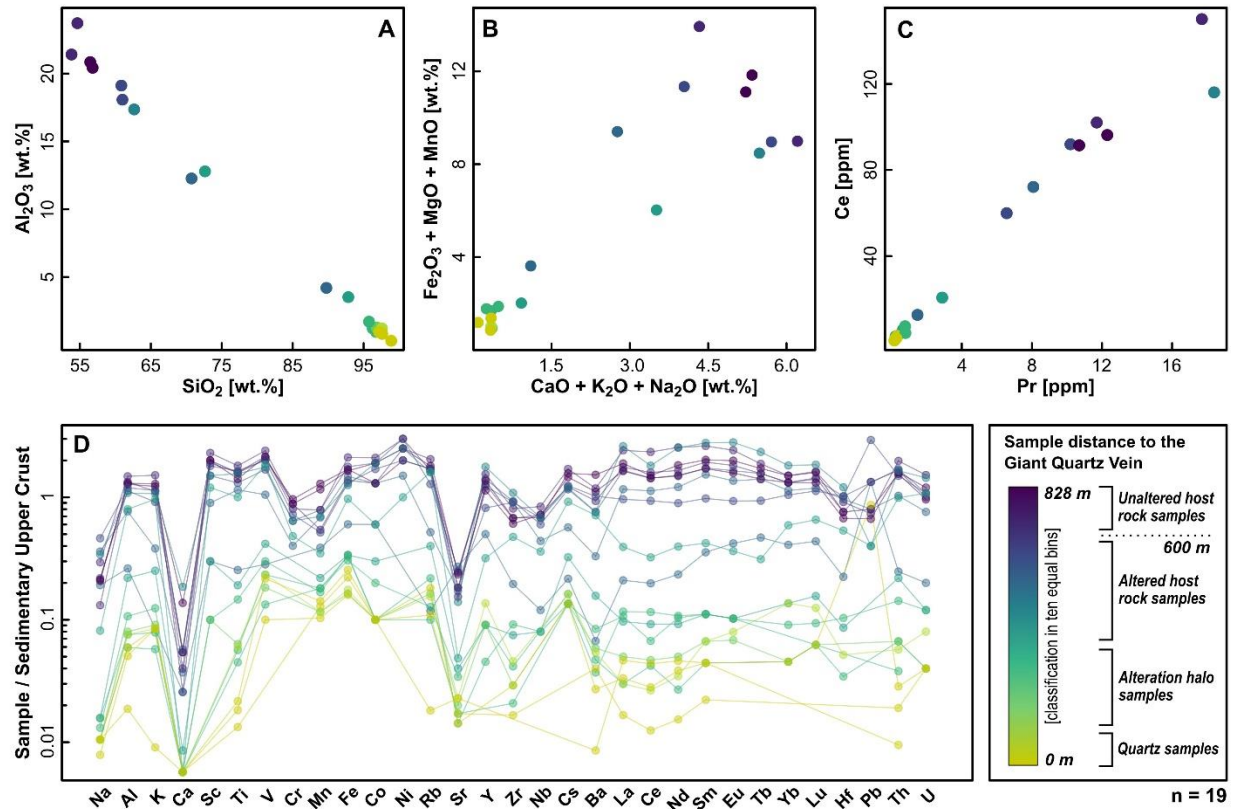


Figure 4. Whole-rock geochemical compositions of the investigated samples regarding their distance to the main quartz bodies. (A)  $SiO_2$  vs.  $Al_2O_3$ , (B)  $CaO+K_2O+Na_2O$  vs.  $Fe_2O_3+MgO+MnO$ , and (C) Pr vs. Ce diagrams. (D) Major and trace element concentrations normalized to the average composition of the sedimentary upper crust [Taylor and McLennan \(1981\)](#). See raw data in the SM2.

## 5 DISCUSSION

### 5.1 Effects on chlorite geothermometric calculations

The six texturally distinct chlorite types show consistent and progressive variations in their chemical composition, revealing mass transfer processes. Host rock-related Chl<sub>1</sub> (Fig. 2D) and quartz-vein-related Chl<sub>6</sub> (Fig. 2G) chlorites represent textural and compositional endmembers, whilst Chl<sub>2-5</sub> are interpreted as transitional chlorites with physicochemical signatures resulting from a wide variety of processes leading to GQV formation. Accordingly, a progressive chlorite chemical refinement, *i.e.*, the process of removing impurities or incompatible elements from a substance, is proposed. Altogether, the complete chemical evolution of the six types of chlorites (Fig. 3A), parallel to an R3 line, corresponds to a temperature change of chlorite formation for a given chemical environment (the blue lines in Fig. 1 of Bourdelle, 2021). Based on textural and microstructural evidence, primary Chl<sub>1</sub> chlorites predate the formation of the studied GQV because they are linked to the development of S<sub>2</sub> surfaces in the host rocks. These pre-existing chlorites are thus interpreted as progressively dissolved and reprecipitated as Chl<sub>2</sub> to Chl<sub>5</sub> chlorites during fluid-rock interaction (Chl<sub>2</sub>, Chl<sub>4</sub>), pressure-solution creep deformation (Chl<sub>3</sub>), and crack-sealing (Chl<sub>5</sub>) processes leading to GQV formation (Fig. 2D-G). On the contrary, Chl<sub>6</sub> chlorites are interpreted as the latest chlorite type formed during the chemical refinement, as they are petrographically “clean”, inclusion-free, and perfectly euhedral crystals formed under conditions close to equilibrium. This process of chemical refinement agrees with the progressive silica enrichment that shows its maximum concentration in Chl<sub>6</sub> quartz-related chlorites (Fig. 3B), as expected in a chemical system giving rise to the formation of a GQV with no other accessory mineral phases. It should be emphasized that all the thermodynamic and semi-empirical chlorite geothermometers assume SiO<sub>2</sub> in excess in the system, hence the activity of SiO<sub>2</sub> cannot influence

the Si content of chlorite; this is only determined by the extent of their tchermack and di-trioctahedral substitutions, that is, by the Al/Fe+Mg ratio in the chlorite composition, which, in turn, is a consequence of temperature, being these two substitutions the ultimate basis of chlorite geothermometry (Vidal et al., 2016).

Given the internal coherence of the obtained dataset, a complete record of the spatiotemporal thermal evolution of chemical chlorite refinement and GQV formation can be inferred from geothermometric calculations. Thermometers that either do not consider (Bourdelle et al., 2013; Lanari et al., 2014; Inoue et al., 2018; Fig. 5A) or consider (Lanari et al., 2014; Inoue et al., 2018; Fig. 5B, C) the Fe<sup>3+</sup> content of chlorite have been applied to determine temperature variations during these processes. If the Fe<sup>3+</sup> content is not considered, the calculated temperatures progressively decrease from host rock-controlled (ca. 300-350°C) to vein quartz-related chlorites (ca. 150-200°C) (Fig. 5A; SM2). A range of Fe<sup>3+</sup>/Fe<sup>T</sup> values was assumed for the Fe<sup>3+</sup>-dependent thermometers (Fig. 5B, C; SM2) to test if these variations are apparent and inferred from the selective incorporation of Fe<sup>3+</sup> during Al-free di-trioctahedral substitution in some chlorite types (e.g., Trincal and Lanari, 2016). The results reveal that the calculated temperatures vary up to 100°C when different Fe<sup>3+</sup>/Fe<sup>T</sup> ratios are considered for each chlorite type. However, there are no common temperatures for all types, even when the typical error of the geothermometers is considered ( $\pm 30^\circ\text{C}$ ) and extreme Fe<sup>3+</sup>/Fe<sup>T</sup> ratios are compared (e.g., 0.05 vs. 0.45) (Fig. 5B, C). Moreover, to assume that the steady decrease of temperature is an artefact due to progressive increase of the proportion of the Fe<sup>3+</sup>/Fe<sup>T</sup> ratios (that is, a horizontal line in Figs. 5B, C) it would be necessary to assume a constant change of the redox potential of the system towards more oxidizing conditions (Vidal et al., 2016), which is an unlikely scenario in a chemically simple system.

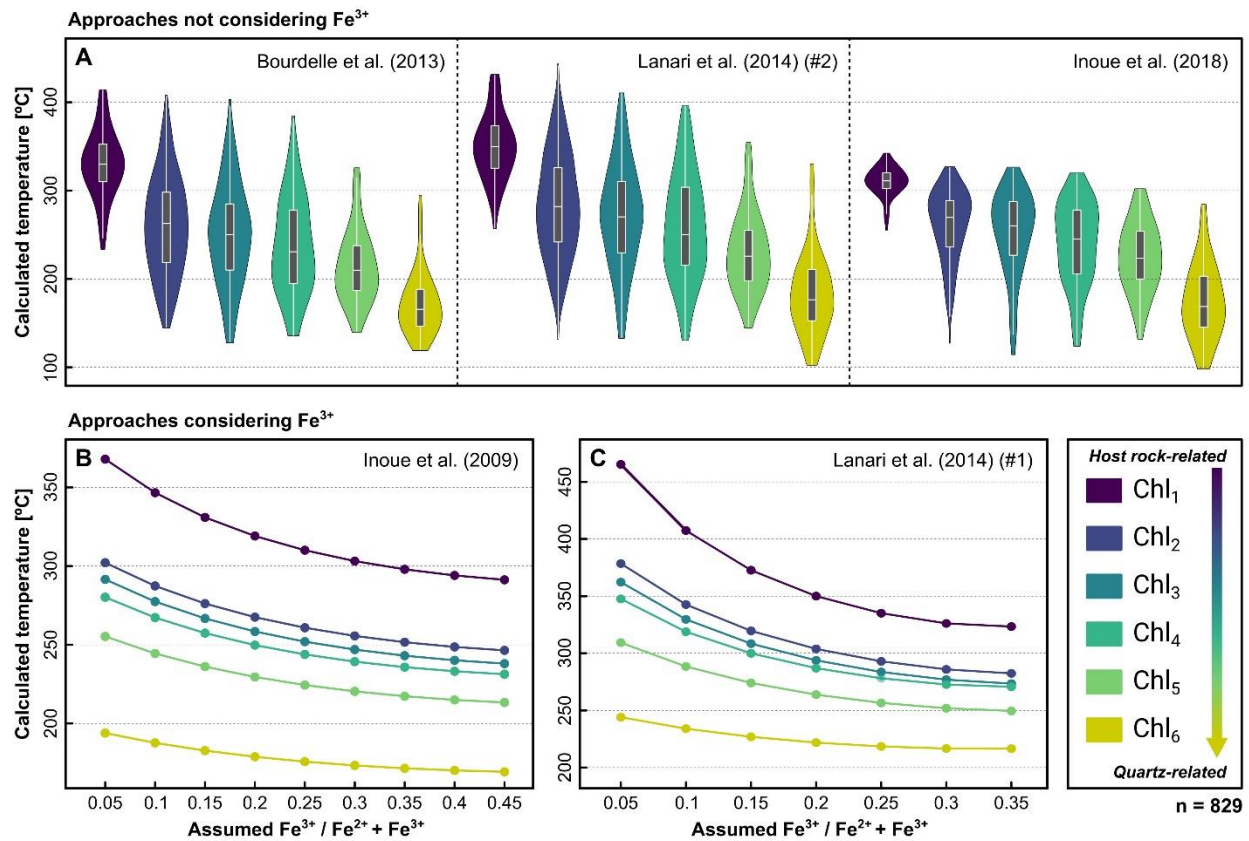


Figure 5. Calculated chlorite temperatures following Fe<sup>3+</sup>-independent (Bourdelle et al., 2013; Lanari et al., 2014; Inoue et al., 2018) (A) and Fe<sup>3+</sup>-dependent (Lanari et al., 2014; Inoue et al., 2018) (B, C) approaches. Horizontal dashed lines represent constant temperatures. See raw data in the SM2.

The results indicate that chlorites that have grown within the same tectonic environment, sometimes even within the same thin section, show different chemical compositions and temperatures depending on the process that controlled their growth (Fig. 2, 3). Therefore, a thorough textural differentiation of chlorite assemblages must be done prior to any analysis, as is common practice for fluid inclusion investigations, in order to finely discriminate groups of chlorites that were formed at the same time (and, thus, under the same temperature conditions; Fig. 3; S5, S6). Furthermore, iron speciation should be considered as a potential source of bias. Despite the lack of effect on the temperatures calculated in this work (Fig. 6B, C), it may result in apparent, unreliable temperatures in other growth environments (Masci et al., 2019). The analysis of iron speciation with an EMP or its calculation based on charge balance is, however, unattainable with the current analytical procedures and not possible for those minerals having structural positions with variable cation totals, and thus requires other analytical techniques (*e.g.*, Mossbauer Spectroscopy or X-ray absorption near-edge spectroscopy; *e.g.*, Forshaw and Pattison, 2021). Modelling different possible values of  $\text{Fe}^{3+}/\text{Fe}^{2+}+\text{Fe}^{3+}$  and evaluating the reliability of the obtained temperatures within the framework of the studied chemical system can be, as demonstrated here, diagnostic of the Fe speciation and redox potential during chlorite growth (Fig. 6B, C). Finally, techniques based on chlorite empirical thermometry should definitely be abandoned in favour of modern, open-source semi-empirical and thermodynamic approaches. The latter methods have demonstrated their robustness when applied coupled to other, independent geothermometric method (*e.g.*, Raman spectroscopy of carbonaceous material, illite crystallinity, pseudosection modelling, and oxygen isotope fractionation), yielding similar results that are further consistent

with the tectono-thermal setting of the investigated regions (*e.g.*, Lacroix et al., 2012; Miron et al., 2013; Rajič et al., 2023).

## 5.2 Implications for Giant Quartz Vein formation

GQVs, sometimes also referred to as giant quartz reefs or quartz lodes, are large (mappable, *e.g.*, at the 1:25,000 scale; Fig. S3) structures that occur in different tectonic settings worldwide. The main noteworthy fact about GQVs is their abnormal dimensions and, therefore, the large amounts of quartz that their formation requires (ca.  $7.5 \cdot 10^9$  kg of quartz for each of the GQVs studied in this work; estimated from maps, assuming a vertical extent of 1/3 the outcropping horizontal length, and a quartz density of  $2.65\text{g/cm}^3$ ). There are three main aspects that are nowadays subject of debate regarding the origin and significance of GQVs: the source of silica, the fluid transport modes driving the mobilisation of that silica, and the time span required for its transport and precipitation (Jia and Kerrich, 2000; Bons, 2001; Sharp et al., 2005; Lemarchand et al., 2012; Tannock et al., 2020; González-Esvertit et al., 2022a, 2022b; Rout et al., 2022). Moreover, further implications of GQVs formation mechanisms and their timescales include the Archean to Phanerozoic orogenic gold deposits with which they may be associated (Goldfarb et al., 2001), and the fluid, heat, and mass transport, as well as the rheological changes in crustal rocks at seismogenic depths that their formation may involve (Fisher and Brantley, 2014; Saishu et al., 2017; Williams and Fagereng, 2022).

Temperatures obtained in the present work (Fig. 5A) indicate that each chlorite type records the temperature of the process that dominated during their formation (Fig. 2D-G, 5). Accordingly, an overall system cooling of more than  $100^\circ\text{C}$  during GQV formation is deduced from quartz-related chlorite types (Chl<sub>2-6</sub>) (Fig. 5). Moreover, the gradual silica enrichment observed in the host rocks

suggests strong fluid-rock interactions and progressive precipitation of quartz, increasing from more than 600 m far towards the sectors where GQVs nucleated (Fig. 4). This is in agreement with those conditions expected for fluid transport regimes under low fluid/rock ratios, where fluids and host rocks are thermally equilibrated (Fisher and Brantley, 1992; Sharp et al., 2005), and could further explain the replacement textures and Si-metasomatism reported in other sectors of the Pyrenees where GQVs are also present (e.g., in the Canigó, Roc de Frausa, and Cap de Creus Massifs; Fig. 1; González-Esvertit et al., 2022b).

The texturally constrained and spatially resolved multiscale geochemical evidence suggest that hydrothermal fluid flow heated up the system prior to rock-buffered reactions and silicification processes. Silica was unlikely derived from magmatic fluids during granitoid formation nor from metamorphic fluids devolatilization, since GQVs in the Pyrenees are also hosted by granites itself or by sedimentary cover rocks that were formed more than 200Ma after the Variscan regional metamorphism and late-Variscan magmatism (González-Esvertit et al., 2022a). Moreover, this unlikely scenario may imply much higher formation temperatures, as well as the presumable occurrence of quartz-hosted CO<sub>2</sub>-rich fluid inclusions and other mineral phases than quartz, which are absent in the GQVs of the Pyrenees (Ayora and Casas, 1983). Accordingly, silica dissolution in deeper metasedimentary host rocks could have been favoured by high dislocation densities and small grain sizes at quartz-mica interfaces (e.g., Renard et al., 1997; Wangen and Munz, 2004) (Figs. 2D-F, S6). The combination of both fluid transport modes, i.e., external advective fluid supplying heat to the system but also locally-derived, rock-buffered fluid and mass transport inferred from widespread fluid-rock alterations, is proposed as the main formation mechanism of the studied GQVs. This process would have taken place during long-lasting, continuous or successive pulses, of heat, fluid, and mass supply, in order to give rise to the strong rock alteration

haloes, involving silicification and replacement, that are found associated to GQVs (González-Esvertit et al., 2022b).

Furthermore, the results suggest that GQVs can be formed at significantly lower temperatures than previously thought (<200°C; Fig. 5). This fact, as well as the suggested silica sources and combination of fluid transport modes, are in disagreement with those statements claiming that GQVs are exclusively formed from extremely large volumes of hot (250-400°C) fluids under high water/rock ratios (e.g., Kerrich and Feng, 1992; Tannock et al., 2020). At the lower temperatures obtained, quartz solubility is also significantly lower (Rimstidt, 1997). Therefore, fluid-rock interactions would have taken place over a longer period of time to form a single GQV composed of  $7.5 \cdot 10^9$  kg of quartz, which is at the bottom end of the spectrum if one considers other GQVs with significantly higher widths and lengths (e.g., in other sectors of the Pyrenees or in the Bundelkhand Craton, India; Rout et al., 2022). The results also have implications in terms of the quartz cementation mechanisms controlling the strength recovery of rocks between earthquakes at seismogenic depths (e.g., Sibson, 1992). Indirect constraints on quartz precipitation rates indicate a long-lasting GQV growth history through continuous or successive pulses. These cementation timescales would be difficult to reconcile with the timescales of the seismic cycle, as also suggested for other quartz precipitation mechanisms occurring at earthquake nucleation temperatures (150-350°C) (see a review in Williams and Fagereng, 2022).

From a regional perspective, the results provide new insights into the tectono-thermal evolution of the Pyrenees and open new questions on the presumed age of the GQVs, whose formation has been hitherto attributed to the Variscan orogeny (Cirés et al., 1994; Carreras et al., 2006; IGME-BRGM, 2009). Chl<sub>1</sub> chlorites, formed coevally to the S<sub>2</sub> cleavage and predating the GQVs development, yielded temperatures of ca. 300-350°C (Fig. 5). These are very similar to temperature conditions

for the Variscan metamorphism and S<sub>2</sub> development obtained with other methods for the same metasedimentary rock successions in neighbouring areas. By means of illite crystallinity, [Bons \(1989\)](#) determined that the Cambrian-Ordovician rocks of the Rabassa dome (western continuation of the study area) were metamorphosed in upper anchizone conditions, roughly corresponding to paleotemperatures between 250°C and 300°C. Using Raman spectroscopy of carbonaceous material, [Cochelin et al. \(2018\)](#) estimated palaeotemperatures around 350°C in the Orri dome (southern continuations of the study area). However, the obtained GQV formation temperatures (<200°C; [Fig. 4](#)) are difficult to reconcile with the Variscan tectono-thermal evolution of the basement rocks of the Pyrenees. Accordingly, the formation of GQVs in the southern slope of the Canigó Massif would fit better in Alpine times, linked to thrust development and basement exhumation, as already constrained by structural analysis ([González-Esvertit et al., 2023](#); [Margalef et al., 2023](#)).

## **6 CONCLUDING REMARKS**

The chemical composition and formation temperature of chlorite may vary dramatically within the same growth environment, potentially leading to petrogenetic misinterpretations when different chlorite groups are not finely discriminated. We demonstrate that one can take advantage of this chemical variability if the analyses are texturally constrained and based on detailed field and petrographic groundwork. For the case study used in this work, petrographic discriminations have allowed describing a gradual process of textural and chemical evolution, named chlorite chemical refinement, related to the formation of giant quartz veins. By coupling this process with spatially resolved elemental concentrations we suggest that giant quartz veins can be formed from rock-buffered fluids involving local mass transport and at lower temperatures than previously thought.

This has allowed us to discuss the sources of silica, fluid transport modes, and timescales involved in giant quartz vein formation, which have been subject of debate during the past years. The results have further implications for the fluid, heat, and mass transfer and quartz cementation mechanisms occurring in the Earth's crust, as well as for the age and significance of the GQVs present in the basement rocks of the Pyrenees and many other localities worldwide.

## ACKNOWLEDGMENTS

We appreciate helpful and constructive suggestions made by Brendan Murphy, Ake Fagereng, Rob Strachan, Joseph Biasi and one anonymous reviewer. This work was funded by DGICYT Projects PID2021-122467NB-C22 and PID2021-125585NB-I00 (MCIU/AEI/FEDER-UE/10.13039/501100011033) and PID2020-118999GB-I00 (MCIN/AEI/10.13039/501100011033), and by the Sedimentary Geology Research Group (2021 SGR 00349). EGE was funded by the Geological Society of London, the PhD grant 2022 FI\_B1 00043 (Generalitat de Catalunya; European Social Fund), and the “Consolidación Investigadora” Grant CNS2022-135819 funded by MCIN/AEI/10.13039/501100011033. EGR was funded by the MCIU/AEI/ESF/10.13039/501100011033 “Ramón y Cajal” fellowship (RYC2018-026335-I).

## SUPPLEMENTARY MATERIAL

<sup>1</sup>Supplemental Material. (1) Summary of the historic and current use of chlorite thermometry, extended methods description, geological setting of the study area, and thin section petrography. (2) Raw data from punctual chlorite and whole-rock geochemical analyses, and statistic summary of the results.

## REFERENCES

- Aguilar, C., Liesa, M., Castiñeiras, P., Navidad, M., 2014. Late Variscan metamorphic and magmatic evolution in the eastern Pyrenees revealed by U–Pb age zircon dating. *Journal of the Geological Society* 171, 181–192. <https://doi.org/10.1144/jgs2012-086>
- Anderson, J.L., Barth, A.P., Wooden, J.L., Mazdab, F., 2008. Thermometers and Thermobarometers in Granitic Systems. *Reviews in Mineralogy and Geochemistry* 69, 121–142. <https://doi.org/10.2138/rmg.2008.69.4>
- Ayora, C., Casas, J.M., 1983. Estudi microtermomètric dels filons de quars de les Esquerdes de Rojà, Massís de Canigó, Pirineu Oriental. *Acta Geologica Hispanica* 18, 35–46.
- Bons, A.J., 1989. Very low-grade metamorphism of the Seo formation in the Orri Dome, South-Central Pyrénées. *Geologie En Mijnbouw* 68, 303–312.

- Bons, A.J., 1988. Intracrystalline Deformation and Slaty Cleavage Development in Very Low-grade Slates from the Central Pyrenees. Instituut voor Aardwetenschappen der Rijksuniversiteit Utrecht.
- Bons, P.D., 2001. The formation of large quartz veins by rapid ascent of fluids in mobile hydrofractures. *Tectonophysics* 336, 1–17. [https://doi.org/10.1016/S0040-1951\(01\)00090-7](https://doi.org/10.1016/S0040-1951(01)00090-7)
- Bons, P.D., Cao, D., Riese, T. de, González-Esvertit, E., Koehn, D., Naaman, I., Sachau, T., Tian, H., Gomez-Rivas, E., 2022. A review of natural hydrofractures in rocks. *Geological Magazine* 159, 1–26. <https://doi.org/10.1017/S0016756822001042>
- Bourdelle, F., 2021. Low-Temperature Chlorite Geothermometry and Related Recent Analytical Advances: A Review. *Minerals* 11, 130. <https://doi.org/10.3390/min11020130>
- Bourdelle, F., Beyssac, O., Parra, T., Chopin, C., 2018. Nanoscale chemical zoning of chlorite and implications for low-temperature thermometry: Application to the Glarus Alps (Switzerland). *Lithos* 314–315, 551–561. <https://doi.org/10.1016/j.lithos.2018.06.030>
- Bourdelle, F., Cathelineau, M., 2015. Low-temperature chlorite geothermometry: a graphical representation based on a T–R<sub>2</sub>–Si diagram. *European Journal of Mineralogy* 27, 617–626. <https://doi.org/10.1127/ejm/2015/0027-2467>
- Bourdelle, F., Parra, T., Chopin, C., Beyssac, O., 2013. A new chlorite geothermometer for diagenetic to low-grade metamorphic conditions. *Contributions to Mineralogy and Petrology* 165, 723–735.
- Brown, M., 1995. P–T–t evolution of orogenic belts and the causes of regional metamorphism. Geological Society, London, *Memoirs* 16, 67–81. <https://doi.org/10.1144/GSL.MEM.1995.016.01.09>
- Carreras, J., Losantos, M., Palau, J., Escuer, J., 2006. Memoria asociada al mapa de la hoja 259 (Rosas) del Mapa Geológico de España. Instituto Geológico y Minero de España (IGME) - Serie MAGNA50.
- Casas, J.M., 2010. Ordovician deformations in the Pyrenees: new insights into the significance of pre-Variscan ('sardic') tectonics. *Geological Magazine* 147, 674–689. <https://doi.org/10.1017/S0016756809990756>
- Chapman, D.S., 1986. Thermal gradients in the continental crust. Geological Society, London, *Special Publications* 24, 63–70. <https://doi.org/10.1144/GSL.SP.1986.024.01.07>
- Cirés, J., Morales, V., Liesa, M., Carreras, J., Escuer, J., Pujadas, J., 1994. Mapa geológico y Memoria de la Hoja nº 220 (La Jonquera). Mapa Geológico de España E. 1:200.000 IGME.
- Cochelin, B., Lemirre, B., Denèle, Y., de Saint Blanquat, M., Lahfid, A., Duchêne, S., 2018. Structural inheritance in the Central Pyrenees: the Variscan to Alpine tectonometamorphic evolution of the Axial Zone. *Journal of the Geological Society* 175, 336–351. <https://doi.org/10.1144/jgs2017-066>
- de Caritat, P., Hutcheon, I., Walshe, J.L., 1993. Chlorite Geothermometry: A Review. *Clays and Clay Minerals* 41, 219–239. <https://doi.org/10.1346/CCMN.1993.0410210>
- Essene, E.J., Peacor, D.R., 1995. Clay Mineral Thermometry—A Critical Perspective. *Clays and Clay Minerals* 43, 540–553. <https://doi.org/10.1346/CCMN.1995.0430504>
- Fall, A., Bodnar, R.J., 2018. How Precisely Can the Temperature of a Fluid Event be Constrained Using Fluid Inclusions? *Economic Geology* 113, 1817–1843. <https://doi.org/10.5382/econgeo.2018.4614>
- Fisher, D.M., Brantley, S.L., 2014. The role of silica redistribution in the evolution of slip instabilities along subduction interfaces: Constraints from the Kodiak accretionary

- complex, Alaska. *Journal of Structural Geology, Fluids and Structures in Fold and Thrust Belts with Recognition of the Work of David V. Wiltschko* 69, 395–414. <https://doi.org/10.1016/j.jsg.2014.03.010>
- Fisher, D.M., Brantley, S.L., 1992. Models of quartz overgrowth and vein formation: Deformation and episodic fluid flow in an ancient subduction zone. *Journal of Geophysical Research* 97, 20043. <https://doi.org/10.1029/92JB01582>
- Forshaw, J.B., Pattison, D.R.M., 2021. Ferrous/ferric (Fe<sup>2+</sup>/Fe<sup>3+</sup>) partitioning among silicates in metapelites. *Contributions to Mineralogy and Petrology* 176, 63. <https://doi.org/10.1007/s00410-021-01814-4>
- Fyfe, W.S., Turner, F.J., Verhoogen, J., 1958. Metamorphic reactions and metamorphic facies. *Geological Society of America Memoirs*. Geological Society of America, 1–251. <https://doi.org/10.1130/MEM73-p1>
- Goldfarb, R.J., Groves, D.I., Gardoll, S., 2001. Orogenic gold and geologic time: a global synthesis. *Ore Geology Reviews* 18, 1–75. [https://doi.org/10.1016/S0169-1368\(01\)00016-6](https://doi.org/10.1016/S0169-1368(01)00016-6)
- Goldstein, R.H., 2001. Fluid inclusions in sedimentary and diagenetic systems. *Lithos, Fluid Inclusions: Phase Relationships - Methods - Applications*. A Special Issue in Honour of Jacques Touret 55, 159–193. [https://doi.org/10.1016/S0024-4937\(00\)00044-X](https://doi.org/10.1016/S0024-4937(00)00044-X)
- Gomez-Rivas, E., Butler, R.W.H., Healy, D., Alsop, I., 2020. From hot to cold - The temperature dependence on rock deformation processes: An introduction. *Journal of Structural Geology* 132, 103977. <https://doi.org/10.1016/j.jsg.2020.103977>
- González-Esvertit, E., Canals, À., Bons, P.D., Casas, J.M., Gomez-Rivas, E., 2022a. Compiling regional structures in geological databases: The giant quartz veins of the Pyrenees as a case study. *Journal of Structural Geology* 163, 104705. <https://doi.org/10.1016/j.jsg.2022.104705>
- González-Esvertit, E., Canals, À., Bons, P.D., Murta, H., Casas, J.M., Gomez-Rivas, E., 2022b. Geology of giant quartz veins and their host rocks from the Eastern Pyrenees (Southwest Europe). *Journal of Maps* 19, 1–13. <https://doi.org/10.1080/17445647.2022.2133642>
- González-Esvertit, E., Molins-Vigatà, J., Canals, À., Casas, J.M., 2023. The geology of the Gréixer area (La Cerdanya, Eastern Pyrenees): Sardinic, Variscan, and Alpine imprints. *Trabajos de Geología* 37(37), 81–95. <https://doi.org/10.17811/tdg.37.2023.81-95>
- Hirth, G., Tullis, J., 1992. Dislocation creep regimes in quartz aggregates. *Journal of Structural Geology* 14, 145–159. [https://doi.org/10.1016/0191-8141\(92\)90053-Y](https://doi.org/10.1016/0191-8141(92)90053-Y)
- Holland, H.D., 1965. Some applications of thermochemical data to problems of ore deposits; [Part] 2, Mineral assemblages and the composition of ore forming fluids. *Economic Geology* 60, 1101–1166. <https://doi.org/10.2113/gsecongeo.60.6.1101>
- IGME-BRGM, 2009. Mapa Geológico de Pirineos 1:400.000.
- Inoue, A., Inoué, S., Utada, M., 2018. Application of chlorite thermometry to estimation of formation temperature and redox conditions. *Clay Minerals* 53, 143–158. <https://doi.org/10.1180/clm.2018.10>
- Jia, Y., Kerrich, R., 2000. Giant quartz vein systems in accretionary orogenic belts: the evidence for a metamorphic fluid origin from N15N and N13C studies. *Earth and Planetary Science Letters* 14.
- Kerrich, R., Feng, R., 1992. Archean geodynamics and the Abitibi-Pontiac collision: implications for advection of fluids at transpressive collisional boundaries and the origin of giant quartz

- vein systems. *Earth-Science Reviews* 32, 33–60. [https://doi.org/10.1016/0012-8252\(92\)90011-H](https://doi.org/10.1016/0012-8252(92)90011-H)
- Koehn, D., Rood, M.P., Beaudoin, N., Chung, P., Bons, P.D., Gomez-Rivas, E., 2016. A new stylolite classification scheme to estimate compaction and local permeability variations. *Sedimentary Geology* 346, 60–71. <https://doi.org/10.1016/j.sedgeo.2016.10.007>
- Lacroix, B., Charpentier, D., Buatier, M., Vennemann, T., Labaume, P., Adate, T., Travé, A., Dubois, M., 2012. Formation of chlorite during thrust fault reactivation. Record of fluid origin and P–T conditions in the Monte Perdido thrust fault (southern Pyrenees). *Contributions to Mineralogy and Petrology* 163, 1083–1102. <https://doi.org/10.1007/s00410-011-0718-0>
- Lanari, P., Wagner, T., Vidal, O., 2014. A thermodynamic model for di-trioctahedral chlorite from experimental and natural data in the system MgO–FeO–Al<sub>2</sub>O<sub>3</sub>–SiO<sub>2</sub>–H<sub>2</sub>O: applications to P–T sections and geothermometry. *Contributions to Mineralogy and Petrology* 167, 968. <https://doi.org/10.1007/s00410-014-0968-8>
- Lemarchand, J., Boulvais, P., Gaboriau, M., Boiron, M.-C., Tartèse, R., Cokkinos, M., Bonnet, S., Jégouzo, P., 2012. Giant quartz vein formation and high-elevation meteoric fluid infiltration into the South Armorican Shear Zone: geological, fluid inclusion and stable isotope evidence. *Journal of the Geological Society* 169, 17–27. <https://doi.org/10.1144/0016-76492010-186>
- Margalef, A., Granado, P., Casas, J.M., 2023. Superposed Variscan and Alpine deformation in the basement rocks of southern Andorra, Central Pyrenees. *Journal of the Geological Society* 0, jgs2023-099. <https://doi.org/10.1144/jgs2023-099>
- Masci, L., Dubacq, B., Verlaquet, A., Chopin, C., De Andrade, V., Herviou, C., 2019. A XANES and EPMA study of Fe<sup>3+</sup> in chlorite: Importance of oxychlorite and implications for cation site distribution and thermobarometry. *American Mineralogist* 104, 403–417. <https://doi.org/10.2138/am-2019-6766>
- Menegon, L., Fagereng, Å., 2021. Tectonic pressure gradients during viscous creep drive fluid flow and brittle failure at the base of the seismogenic zone. *Geology* 49, 1255–1259. <https://doi.org/10.1130/G49012.1>
- Miron, G.D., Wagner, T., Wälle, M., Heinrich, C.A., 2013. Major and trace-element composition and pressure–temperature evolution of rock-buffered fluids in low-grade accretionary-wedge metasediments, Central Alps. *Contributions to Mineralogy and Petrology* 165, 981–1008. <https://doi.org/10.1007/s00410-012-0844-3>
- Muñoz, J.A., 1992. Evolution of a continental collision belt: ECORS-Pyrenees crustal balanced cross-section. In: McClay, K.R. (Ed.), *Thrust Tectonics*. Springer Netherlands, Dordrecht, 235–246. [https://doi.org/10.1007/978-94-011-3066-0\\_21](https://doi.org/10.1007/978-94-011-3066-0_21)
- Navidad, M., Castiñeiras, P., Casas, J.M., Liesa, M., Belousova, E., Proenza, J., Aiglsperger, T., 2018. Ordovician magmatism in the Eastern Pyrenees: Implications for the geodynamic evolution of northern Gondwana. *Lithos* 314–315, 479–496. <https://doi.org/10.1016/j.lithos.2018.06.019>
- Padel, M., Clausen, S., Álvaro, J.J., Casas, J.M., 2018. Review of the Ediacaran-Lower Ordovician (pre-Sardic) stratigraphic framework of the Eastern Pyrenees, southwestern Europe. *Geologica Acta* 16, 339–365.
- Pérez-Cáceres, I., Martínez Poyatos, D.J., Vidal, O., Beyssac, O., Nieto, F., Simancas, J.F., Azor, A., Bourdelle, F., 2020. Deciphering the metamorphic evolution of the Pulo do Lobo

- metasedimentary domain (SW Iberian Variscides). *Solid Earth* 11, 469–488. <https://doi.org/10.5194/se-11-469-2020>
- Rajič, K., Raimbourg, H., Lerouge, C., Famin, V., Dubacq, B., Canizarés, A., Di Carlo, I., Maubec, N., 2023. Metamorphic reactions and their implication for the fluid budget in metapelites at seismogenic depths in subduction zones. *Tectonophysics* 857, 229844. <https://doi.org/10.1016/j.tecto.2023.229844>
- Rasmussen, B., Zi, J.-W., Muhling, J.R., Dunkley, D.J., Fischer, W.W., 2020. U-Pb dating of overpressure veins in late Archean shales reveals six episodes of Paleoproterozoic deformation and fluid flow in the Pilbara craton. *Geology* 48, 961–965. <https://doi.org/10.1130/G47526.1>
- Renard, F., Ortoleva, P., Gratier, J.P., 1997. Pressure solution in sandstones: influence of clays and dependence on temperature and stress. *Tectonophysics* 280, 257–266. [https://doi.org/10.1016/S0040-1951\(97\)00039-5](https://doi.org/10.1016/S0040-1951(97)00039-5)
- Rimstidt, J.D., 1997. Quartz solubility at low temperatures. *Geochimica et Cosmochimica Acta* 61, 2553–2558. [https://doi.org/10.1016/S0016-7037\(97\)00103-8](https://doi.org/10.1016/S0016-7037(97)00103-8)
- Roedder, E., 1984. Fluid inclusions. De Gruyter. <https://doi.org/10.1515/9781501508271>
- Rout, D., Panigrahi, M.K., Mernagh, T.P., Pati, J.K., 2022. Origin of the Paleoproterozoic “Giant Quartz Reef” System in the Bundelkhand Craton, India: Constraints from Fluid Inclusion Microthermometry, Raman Spectroscopy, and Geochemical Modelling. *Lithosphere* 2022, 3899542. <https://doi.org/10.2113/2022/3899542>
- Saishu, H., Okamoto, A., Otsubo, M., 2017. Silica precipitation potentially controls earthquake recurrence in seismogenic zones. *Scientific Reports* 7, 13337. <https://doi.org/10.1038/s41598-017-13597-5>
- Sharp, Z.D., Masson, H., Lucchini, R., 2005. Stable isotope geochemistry and formation mechanisms of quartz veins; extreme paleoaltitudes of the Central Alps in the Neogene. *American Journal of Science* 305, 187–219. <https://doi.org/10.2475/ajs.305.3.187>
- Sibson, R.H., 1992. Implications of fault-valve behaviour for rupture nucleation and recurrence. *Tectonophysics* 211, 283–293. [https://doi.org/10.1016/0040-1951\(92\)90065-E](https://doi.org/10.1016/0040-1951(92)90065-E)
- Tannock, L., Herwegh, M., Berger, A., Liu, J., Lanari, P., Regenauer-Lieb, K., 2020. Microstructural analyses of a giant quartz reef in south China reveal episodic brittle-ductile fluid transfer. *Journal of Structural Geology* 130, 103911. <https://doi.org/10.1016/j.jsg.2019.103911>
- Taylor, S.R., McLennan, S.M., 1981. The composition and evolution of the continental crust: rare earth element evidence from sedimentary rocks. *Philosophical Transactions of the Royal Society of London. Series A, Mathematical and Physical Sciences* 301, 381–399.
- Torgersen, E., Viola, G., 2014. Structural and temporal evolution of a reactivated brittle–ductile fault – Part I: Fault architecture, strain localization mechanisms and deformation history. *Earth and Planetary Science Letters* 407, 205–220. <https://doi.org/10.1016/j.epsl.2014.09.019>
- Trincal, V., Lanari, P., 2016. Al-free di-trioctahedral substitution in chlorite and a ferri-sudoite end-member. *Clay Minerals* 51, 675–689. <https://doi.org/10.1180/claymin.2016.051.4.09>
- Uno, M., Okamoto, A., Akatsuka, T., Tsuchiya, N., 2023. Continuous thermal structures of the present-day and contact-metamorphic geothermal systems revealed by drill cuttings in the Kakkonda geothermal field, Japan. *Geothermics* 115, 102806. <https://doi.org/10.1016/j.geothermics.2023.102806>

- Valley, J.W., 2001. Stable Isotope Thermometry at High Temperatures. *Reviews in Mineralogy and Geochemistry* 43, 365–413. <https://doi.org/10.2138/gsrmg.43.1.365>
- Verdecchia, S.O., Collo, G., Zandomeni, P.S., Wunderlin, C., Fehrmann, M., 2019. Crystallochemical indexes and geothermobarometric calculations as a multiproxy approach to P-T condition of the low-grade metamorphism: The case of the San Luis Formation, Eastern Sierras Pampeanas of Argentina. *Lithos* 324–325, 385–401. <https://doi.org/10.1016/j.lithos.2018.11.021>
- Vidal, O., Lanari, P., Munoz, M., Bourdelle, F., De Andrade, V., 2016. Deciphering temperature, pressure and oxygen-activity conditions of chlorite formation. *Clay Minerals* 51, 615–633. <https://doi.org/10.1180/claymin.2016.051.4.06>
- Wagner, T., Cook, N.J., 2000. Late-orogenic alpine-type (apatite)-quartz fissure vein mineralization in the Rheinisches Schiefergebirge, NW Germany: mineralogy, formation conditions and lateral-secretionary origin. *Mineralogical Magazine* 64, 539–560. <https://doi.org/10.1180/002646100549418>
- Wangen, M., Munz, I.A., 2004. Formation of quartz veins by local dissolution and transport of silica. *Chemical Geology*, 209 (3-4). <https://doi.org/10.1016/j.chemgeo.2004.02.011>
- Warr, L.N., 2021. IMA–CNMNC approved mineral symbols. *Mineralogical Magazine* 85, 291–320. <https://doi.org/10.1180/mgm.2021.43>
- Wilkinson, J.J., Chang, Z., Cooke, D.R., Baker, M.J., Wilkinson, C.C., Inglis, S., Chen, H., Bruce Gemmill, J., 2015. The chlorite proximator: A new tool for detecting porphyry ore deposits. *Journal of Geochemical Exploration* 152, 10–26. <https://doi.org/10.1016/j.gexplo.2015.01.005>
- Williams, R.T., Fagereng, Å., 2022. The Role of Quartz Cementation in the Seismic Cycle: A Critical Review. *Reviews of Geophysics* 60. <https://doi.org/10.1029/2021RG000768>